

Preparation and Characterization of Rhodium(III) Complexes Containing (2-Aminoethyl)dimethylphosphine (edmp) or 1,2-Bis(dimethylphosphino)ethane (dmpe). Structures of *fac*-[Rh(edmp)₃]³⁺, *trans*(Cl, Cl), *cis*(P, P)-[RhCl₂(edmp)₂]⁺, and *trans*-[RhCl₂(dmpe)₂]⁺

Kim P. SIMONSEN,[†] Nahomi SUZUKI,^{††} Masatoshi HAMADA,^{††} Masaaki KOJIMA,
Shigeru OHBA,^{††} Yoshihiko SAITO,^{††} and Junnosuke FUJITA*

Department of Chemistry, Faculty of Science, Nagoya University, Chikusa-ku, Nagoya 464-01

^{††}Department of Chemistry, Faculty of Science and Technology, Keio University, 3-14-1,
Hiyoshi, Kohoku-ku, Yokohama 223

(Received May 12, 1989)

The *fac*-[Rh(edmp)₃]³⁺ (edmp=(2-aminoethyl)dimethylphosphine), *trans*(Cl, Cl), *cis*(P, P)-[RhCl₂(edmp)₂]⁺, and *trans*-[RhCl₂(dmpe)₂]⁺ (dmpe=1,2-bis(dimethylphosphino)ethane) complexes were prepared and the molecular structures were determined by the single crystal X-ray diffraction method. Crystal data and final *R* values are: *fac*-[Rh(edmp)₃]Br₃·3H₂O, orthorhombic, *Pna*2₁, *a*=26.750(4), *b*=10.125(1), *c*=9.592(1) Å, *V*=2598.2(5) Å³, *Z*=4, *R*=0.039 for 1590 observed unique reflections. *trans*(Cl, Cl), *cis*(P, P)-[RhCl₂(edmp)₂]PF₆, monoclinic, *P*2₁/*a*, *a*=18.197(4), *b*=12.574(2), *c*=8.615(1) Å, *β*=96.59(2)°, *V*=1958.2(6) Å³, *Z*=4, *R*=0.032 for 3379 reflections. *trans*(Cl, Cl), *cis*(P, P)-[RhCl₂(edmp)₂]ClO₄, triclinic, *P* $\bar{1}$, *a*=13.122(2), *b*=17.952(2), *c*=12.343(2) Å, *α*=91.65(2), *β*=102.46(2), *γ*=80.74(1)°, *V*=2802.0(7) Å³, *Z*=6, *R*=0.070 for 7513 reflections. *trans*-[RhCl₂(dmpe)₂]CF₃SO₃, monoclinic, *P*2₁/*a*, *a*=13.166(2), *b*=24.337(4), *c*=8.002(2) Å, *β*=95.95(2)°, *V*=2550.1(8) Å³, *Z*=4, *R*=0.040 for 3201 reflections. It was found that the shorter the Rh–P bond length, the larger the *trans* Rh–N bond elongation. The mean Rh–P bond distance in *trans*-[RhCl₂(dmpe)₂]CF₃SO₃ (2.337(2) Å) is longer than those in *fac*-[Rh(edmp)₃]Br₃·3H₂O (2.283(4) Å) and *trans*(Cl, Cl), *cis*(P, P)-[RhCl₂(edmp)₂]PF₆ (2.252(2) Å). A series of complexes of *trans*(X, X), *cis*(P, P)-[RhX₂(edmp)₂]⁺ (X=Cl, Br, I) and *trans*-[RhX₂(dmpe)₂]⁺ (X=Cl, Br) were also prepared and their absorption spectra were compared with one another and with those of the corresponding cobalt(III) complexes.

In a previous paper,¹⁾ we reported the preparation of *trans*(Cl, Cl), *cis*(P, P) and *cis*(Cl, Cl), *trans*(P, P) isomers of [RhCl₂(edpp)₂]⁺, where edpp denotes (2-aminoethyl)diphenylphosphine. The X-ray analyses of the complexes revealed the *trans* influence of P donor atoms on the Rh–N and Rh–P bond lengths. (2-Aminoethyl)dimethylphosphine (edmp) has less bulky substituents on the phosphorus atom than does edpp, and it is interesting to see the steric and electronic effects of the substituent on P on such properties as *trans* influence.

This paper describes the preparation and X-ray structure analyses of *fac*-[Rh(edmp)₃]³⁺, *trans*(Cl, Cl), *cis*(P, P)-[RhCl₂(edmp)₂]⁺, and the related *trans*-[RhCl₂(dmpe)₂]⁺ complex. A series of complexes of *trans*(X, X), *cis*(P, P)-[RhX₂(edmp)₂]⁺ (X=Cl, Br, I) and *trans*-[RhX₂(dmpe)₂]⁺ (X=Cl, Br) were also prepared and their absorption spectra were compared with one another and with those of the corresponding cobalt(III) complexes.

Experimental

The edmp²⁾ and dmpe³⁾ ligands were prepared according to literature methods, and handled under an atmosphere of nitrogen until they formed air-stable rhodium(III) complexes. Absorption, and ¹H and ¹³C NMR spectra were

recorded on a Hitachi 323 spectrophotometer and a Hitachi R-90H spectrometer, respectively.

Preparation of Complexes. *fac*-[Rh(edmp)₃]Cl₃·4H₂O. A deaerated ethanol solution (10 cm³) of RhCl₃·3H₂O (0.40 g, 1.52 mmol) was heated to reflux. To this solution was added a deaerated ethanol solution (7 cm³) of edmp (0.74 g, 7 mmol). The mixture was refluxed for 12 h to give a yellow solution together with a white crystalline solid. The mixture was allowed to cool in an ice bath, and the white crystals were collected by filtration. The crude product was dissolved in water (2 cm³) and filtered. The filtrate was heated and poured into boiling ethanol (25 cm³). The mixture was allowed to stand at room temperature for a while, and then in a freezer overnight to yield white crystals. They were collected by filtration, washed successively with ethanol and diethyl ether, and air dried. Yield: 0.50 g (55%). Found: C, 24.03; H, 7.19; N, 7.05; Cl, 17.94%. Calcd for [Rh(edmp)₃]Cl₃·4H₂O=C₁₂H₄₄N₃Cl₃O₄P₃Rh: C, 24.16; H, 7.43; N, 7.04; Cl, 17.82%. Thermogravimetry: loss of weight 127 mg/g sample, i.e. 76.2 g mol⁻¹. Calcd for [Rh(edmp)₃]Cl₃·4H₂O: 72.1 g mol⁻¹. ¹H NMR (D₂O) δ=1.75–2.05 (18H, four-line multiplet, CH₃), 2.10–2.55 (6H, m, CH₂P), and 2.6–3.5 (6H m, CH₂N). ¹³C NMR (D₂O) δ=13.6 (six-line multiplet, CH₃), 15.2 (six-line multiplet, CH₃), 34.9 (six-line multiplet, CH₂P), and 42.1 (s, CH₂N). The complex is soluble in water and methanol.

fac-[Rh(edmp)₃]Br₃·3H₂O (1). To an aqueous solution (1 cm³) of *fac*-[Rh(edmp)₃]Cl₃·4H₂O (0.10 g, 0.17 mmol) was added a hot aqueous solution (3 cm³) of NaBr (1.5 g). The solution was allowed to stand overnight for crystallization. The colorless crystals were collected by filtration and washed successively with ice-cold water, ethanol, and di-

[†] On leave from Chemistry Department I, University of Copenhagen, Universitetsparken 5, DK-2100, Copenhagen φ, Denmark.

ethyl ether and air dried. Yield: 0.10 g (84% based on the chloride). The structure of the complex was determined by X-ray analysis.

mer-[RhCl₃(P(*n*-Bu)₃)₃]. Attempts to prepare the complex by the published methods^{4,5} did not lead to any crystallization of the complex. The complex was prepared by a modified method of Intille.⁵ A deaerated ethanol solution (10 cm³) containing RhCl₃·3H₂O (0.94 g, 3.6 mmol) and tributylphosphine (4 cm³, 16 mmol) was refluxed for 1.5 h to give an orange solution. The solvent was evaporated off under reduced pressure and the residual orange oil was dissolved in hexane (20 cm³). The solution was then added to water (20 cm³), and hexane was evaporated slowly (1–2 d) at room temperature. The orange crystals deposited were collected by filtration, washed thoroughly with water and dried in a desiccator over P₄O₁₀. Yield: 2.1 g (72%). Found: C, 52.25; H, 10.11%. Calcd for [RhCl₃(P(*n*-Bu)₃)₃]=C₃₆H₈₁Cl₃P₃Rh: C, 52.92; H, 10.00%. The ¹H NMR spectrum was identical with that reported by Intille.⁵

trans(Cl,Cl),cis(P,P)-[RhCl₂(edmp)₂]PF₆ (2a). To a deaerated stirred benzene solution (50 cm³) of *mer*-[RhCl₃(P(*n*-Bu)₃)₃] (1.63 g, 2.0 mmol) was added dropwise edmp (0.53 g, 5.0 mmol). The mixture was refluxed for 1 h to give a yellow precipitate. After cooling for a while, the precipitate was collected on a glass filter by filtration, washed with diethyl ether and dried in a desiccator over P₄O₁₀. The product (ca. 0.9 g) was hygroscopic, mixed with ethanol (50 cm³), and the mixture was filtered to leave a small amount of white crystals on the filter. Yield: 0.04 g. This product was *fac*-[Rh(edmp)₃]Cl₃. The yellow filtrate was evaporated to nearly dryness under reduced pressure, and the residue was redissolved in water (50 cm³). The solution was passed through a short column (ϕ1.0 cm × 3 cm) of SP-Sephadex C-25 in order to remove highly charged species. The yellow eluate was applied on a column (ϕ2.5 cm × 30 cm) of SP-Sephadex C-25. The adsorbed product was eluted with 0.05 mol dm⁻³ NaCl. The eluate containing the fastest-moving yellow main band was collected and evaporated to dryness under reduced pressure. The residue was shaken with ethanol (3 × 20 cm³) to extract the complex, the solvent was evaporated to dryness under reduced pressure, and the residue was dissolved in water (10 cm³). The solution was filtered, heated to 90 °C, and to this solution was added a saturated aqueous solution (4 cm³) of NH₄PF₆. The mixture was allowed to stand at room temperature for a while, and then in a refrigerator overnight to yield yellow crystals. They were collected by filtration, washed successively with ethanol and diethyl ether, and dried in air. Yield: 0.30 g (28%). Found: C, 18.01; H, 4.63; N, 5.32; Cl, 13.27%. Calcd for [RhCl₂(edmp)₂]PF₆=C₈H₂₄N₂Cl₂F₆P₃Rh: C, 18.16; H, 4.57; N, 5.30; Cl, 13.40%. ¹H NMR (C₆D₅NO₂) δ=1.84–1.97 (12H, filled-in-doublet, CH₃), 2.15–2.6 (4H, m, CH₂P), 3.05–3.8 (4H, m, CH₂N), and 4.2–4.65 (4H, br, NH₂). ¹³C NMR (CD₃CN) δ=10.9 (filled-in doublet, CH₃), 32.9 (filled-in doublet, CH₂P), and 40.8 (s, CH₂N). The complex is soluble in acetonitrile, dichloromethane, ethanol, and water. Single crystals suitable for X-ray analysis were obtained by slow evaporation of a methanol solution of the complex.

trans(Cl,Cl),cis(P,P)-[RhCl₂(edmp)₂]ClO₄ (2b). An aqueous solution of *trans*(Cl,Cl),*cis*(P,P)-[RhCl₂(edmp)₂]PF₆ (ca. 0.1 g) was applied on a column of SP-Sephadex C-25. The complex was eluted with 0.1 mol dm⁻³ NaCl, and the eluate

was evaporated to dryness under reduced pressure. The complex was extracted with ethanol, and the solvent was evaporated. The residue was dissolved in water (5 cm³) and to this solution was added a hot solution of LiClO₄ (2 g) in water (2 cm³). The mixture was allowed to stand for crystallization. Single crystals for X-ray analysis were obtained by recrystallization from ethanol.

trans(Br,Br),cis(P,P)-[RhBr₂(edmp)₂]PF₆. This complex was prepared from *trans*(Cl,Cl),*cis*(P,P)-[RhCl₂(edmp)₂]PF₆ and KBr. To a hot aqueous solution (12 cm³) of *trans*(Cl,Cl),*cis*(P,P)-[RhCl₂(edmp)₂]PF₆ (0.1 g, 0.19 mmol) was added a large excess of KBr (5 g, 42 mmol), and the mixture was refluxed for 20 h. The solution was evaporated to dryness under reduced pressure, and the residue was shaken with acetonitrile (ca. 60 cm³) to extract the products until the extracts were colorless. The combined extracts were evaporated to dryness under reduced pressure. The residue was dissolved in water (60 cm³) and the solution was applied on a column (ϕ2.5 cm × 15 cm) of Sp-Sephadex C-25. By elution with 0.05 mol dm⁻³ KBr, two yellow bands developed, the slower-moving one remaining almost at the top of the column. The eluate containing the faster-moving band was collected and evaporated to dryness under reduced pressure. The residue was extracted repeatedly with acetonitrile, and the solvent was removed under reduced pressure. The residue was dissolved in boiling water (10 cm³), and to this solution was added a solution of NH₄PF₆ (0.5 g) in water (2 cm³). The mixture was allowed to stand first at room temperature and then overnight in a refrigerator to yield yellow crystals. They were collected by filtration, washed successively with ice-cold water and diethyl ether, and dried in air. Yield: 0.05 g (43%). Found: C, 15.57; H, 3.89; N, 4.53%. Calcd for [RhBr₂(edmp)₂]PF₆=C₈H₂₄N₂Br₂F₆P₃Rh: C, 15.55; H, 3.91; N, 4.53%.

trans(I,I),cis(P,P)-[RhI₂(edmp)₂]PF₆. This complex was prepared in a similar method to that for the dibromo complex, NaI in ethanol being used instead of KBr and dichloromethane as the extraction solvent. The product was purified by SP-Sephadex C-25 column chromatography (eluent: 0.05 mol dm⁻³ NaI). Yield: 0.06 g (44%, reddish needles). Found: C, 13.49; H, 3.38; N, 3.95%. Calcd for [RhI₂(edmp)₂]PF₆=C₈H₂₄N₂I₂F₆P₃Rh: C, 13.50; H, 3.40; N, 3.94%.

trans-[RhCl₂(dmpe)₂]CF₃SO₃ (3). To a deaerated, boiling ethanol solution (50 cm³) of RhCl₃·3H₂O (0.54 g, 2.05 mmol) was added dropwise dmpe (0.8 g, 5.3 mmol). The mixture was refluxed for 2 h to give a yellow solution together with a small amount of brownish precipitate. After cooling to room temperature, the mixture was filtered, and the filtrate was evaporated to dryness under reduced pressure. The yellow residue was washed with diethyl ether and was dissolved in water (50 cm³). The solution was filtered, and the filtrate was applied on a column (ϕ 2.5 cm × 30 cm) of SP-Sephadex C-25. The rest of the procedure was the same as that for *trans*(Cl,Cl),*cis*(P,P)-[RhCl₂(edmp)₂]PF₆ except that NaCF₃SO₃·H₂O was used instead of NH₄PF₆ for crystallization. Yield: 0.38 g (30%). Found: C, 24.96; H, 5.23; Cl, 11.46; S, 5.82%. Calcd for [RhCl₂(dmpe)₂]CF₃SO₃=C₁₃H₃₂Cl₂F₃O₃SP₄Rh: C, 25.06; H, 5.18; Cl, 11.38; S, 5.14%. ¹H NMR (C₆D₅NO₂) δ=1.65–1.90 (24H, b, CH₃) and 2.0–2.4 (8H, m, CH₂). The complex is soluble in acetonitrile, acetone, ethanol, and methanol, and slightly soluble in water. Yellow needle-like crystals grown from aqueous solution were used for X-ray analysis.

Table 1. Crystal Data, Experimental Conditions, and Refinement Details

	1	2a	2b	3
Chemical formula	[Rh(PC ₄ H ₁₂ N) ₃]- Br ₃ ·3H ₂ O	[RhCl ₂ (PC ₄ H ₁₂ N) ₂]- PF ₆	[RhCl ₂ (PC ₄ H ₁₂ N) ₂]- ClO ₄	[RhCl ₂ (P ₂ C ₆ H ₁₆) ₂]- CF ₃ SO ₃
Formula weight	712.0	528.8	483.5	623.2
Space group	<i>Pna</i> 2 ₁	<i>P</i> 2 ₁ / <i>a</i>	<i>P</i> $\bar{1}$	<i>P</i> 2 ₁ / <i>a</i>
<i>D</i> _m and <i>D</i> _x /Mg m ⁻³	1.78(2), 1.82	—, ^{a)} 1.79	1.70(2), 1.72	1.63(2), 1.62
μ (Mo <i>K</i> α)/mm ⁻¹	5.42	1.79	1.51	1.23
Color of crystals	Colorless	Yellow	Yellow	Yellow
Size of specimen/mm ³	0.36×0.40×0.50	Sphere of 0.45 (5) mm in diameter	0.60×0.43×0.30	0.25×0.25×0.50
Laue group	<i>mmm</i>	2/ <i>m</i>	$\bar{1}$	2/ <i>m</i>
Range of <i>h</i> , <i>k</i> , and <i>l</i>	0≤ <i>h</i> ≤13 0≤ <i>k</i> ≤34 0≤ <i>l</i> ≤12	−23≤ <i>h</i> ≤23 0≤ <i>k</i> ≤16 0≤ <i>l</i> ≤11	−17≤ <i>h</i> ≤17 −23≤ <i>k</i> ≤0 −16≤ <i>l</i> ≤16	−17≤ <i>h</i> ≤17 0≤ <i>k</i> ≤31 0≤ <i>l</i> ≤10
Systematic absences	<i>h</i> 0 <i>l</i> , <i>h</i> odd; 0 <i>k</i> <i>l</i> , <i>k</i> + <i>l</i> odd	<i>h</i> 0 <i>l</i> , <i>h</i> odd; 0 <i>k</i> 0, <i>k</i> odd		<i>h</i> 0 <i>l</i> , <i>h</i> odd; 0 <i>k</i> 0, <i>k</i> odd
Possible space group	<i>Pna</i> 2 ₁ or <i>Pnam</i>	<i>P</i> 2 ₁ / <i>a</i>	<i>P</i> 1 or <i>P</i> $\bar{1}$	<i>P</i> 2 ₁ / <i>a</i>
Variation of five standard reflections	0.99—1.01	0.99—1.01	0.99—1.00	1.00—1.01
$\Sigma(F_o / F_o _{\text{initial}})/5$				
Number of reflections measured	3172	4794	13283	6269
Number of reflections observed [$ F_o /3 > \sigma(F_o)$]	1591	3607	7775	3411
Transmission factor, <i>A</i>	0.121—0.275	0.624—0.628	0.623—0.726	0.718—0.757
Number of unique reflections	1591	3379	7513	3201
Final <i>R</i> value	0.039	0.032	0.070	0.040
(Δ/σ) _{max} for nonhydrogen atoms	0.42	0.50	0.27	0.27
$\Delta\sigma/e \text{ \AA}^{-3}$	−0.93, 0.62	−0.57, 0.35	−1.08, 1.84	−0.62, 0.34

a) *D*_m for **2a** was not measured because almost all of the crystals became opaque gradually in methanol solution and quickly in the air. A transparent part of the crystal was used for X-ray intensity measurement.

Table 2. Fractional Coordinates (×10⁴, ×10⁵ for Rh) and Equivalent Thermal Parameters (×10)

Atom	<i>x</i>	<i>y</i>	<i>z</i>	<i>B</i> _{eq} /(Å ² ×10)	Atom	<i>x</i>	<i>y</i>	<i>z</i>	<i>B</i> _{eq} /(Å ² ×10)
1					2b				
Rh	13627(3)	76919(8)	0 ^{a)}	15	P(2)	1929(1)	1107(1)	1172(1)	33
Br(1)	9923(1)	7411(1)	4962(3)	35	N(1)	−48(2)	3157(3)	531(4)	40
Br(2)	3773(1)	7673(2)	167(2)	45	N(2)	675(2)	1348(3)	−1301(3)	33
Br(3)	7299(1)	7290(2)	3711(2)	41	P	1195(1)	−2780(1)	3560(1)	42
O(1)	8889(4)	8017(9)	6845(13)	47	F(1)	1291(2)	−3688(3)	2322(4)	83
O(2)	784(5)	5413(14)	3815(16)	76	F(2)	2044(2)	−2590(5)	3704(5)	127
O(3)	7133(4)	4131(12)	4253(20)	84	F(3)	1255(2)	−3634(3)	4911(4)	83
P(1)	514(1)	7809(3)	271(4)	20	F(4)	1061(3)	−1892(4)	4686(5)	128
P(2)	1341(1)	5934(3)	−1483(4)	20	F(5)	1090(2)	−1973(2)	2138(4)	70
P(3)	1422(1)	9230(3)	−1731(4)	19	F(6)	343(2)	−3014(4)	3338(5)	96
N(1)	1355(4)	9084(10)	1752(12)	24	C(1)	367(3)	3997(4)	3049(7)	60
N(2)	1457(4)	6206(11)	1587(13)	29	C(2)	1165(3)	2425(4)	4945(5)	52
N(3)	2169(4)	7891(9)	32(16)	24	C(3)	1981(3)	3944(4)	3384(5)	49
C(1)	119(5)	8435(14)	−1088(19)	27	C(4)	1671(3)	143(4)	−386(5)	43
C(2)	185(5)	6353(13)	883(19)	31	C(5)	2823(3)	1654(5)	864(7)	58
C(3)	450(6)	9002(13)	1688(15)	29	C(6)	2125(3)	326(4)	2929(5)	52
C(4)	903(5)	8938(13)	2607(15)	24	C(7)A	46(4)	4195(6)	1463(10)	38
C(5)	789(5)	5559(14)	−2483(17)	29	C(7)B	−266(5)	3605(9)	1968(12)	49
C(6)	1827(6)	5747(13)	−2762(17)	31	C(8)	1313(3)	740(4)	−1779(5)	41
C(7)	1384(6)	4552(12)	−314(14)	22	2b				
C(8)	1689(6)	4943(12)	972(17)	28	Rh(A)	98585(7)	64643(5)	37924(7)	28
C(9)	1259(6)	10887(14)	−1266(18)	34	Rh(B)	43698(6)	63560(5)	−19411(6)	23
C(10)	1149(5)	8963(13)	−3441(17)	29	Rh(C)	25069(7)	99641(5)	23582(7)	33
C(11)	2094(5)	9295(14)	−2052(16)	26	Cl(1)A	10509(3)	7591(2)	4292(3)	46
C(12)	2341(5)	9136(14)	−612(16)	26	Cl(2)A	9249(3)	5304(2)	3457(3)	48
2a					Cl(1)B	5713(2)	5856(2)	−460(2)	39
Rh	9422(1)	21962(2)	8824(3)	23	Cl(2)B	3051(2)	6766(2)	−3494(2)	43
Cl(1)	250(1)	940(1)	2078(1)	42	Cl(1)C	1808(3)	9004(2)	1284(3)	65
Cl(2)	1516(1)	3492(1)	−529(1)	38	Cl(2)C	3273(3)	10959(2)	3298(3)	54
P(1)	1167(1)	3121(1)	3129(1)	30	Cl(3)	4904(2)	3825(2)	−3540(3)	41
					Cl(4)	10751(3)	3181(2)	1711(3)	69

Table 2. (Continued)

Atom	x	y	z	$B_{eq}/(\text{\AA}^2 \times 10)$	Atom	x	y	z	$B_{eq}/(\text{\AA}^2 \times 10)$
Cl(5)	6913(4)	10008(3)	1445(4)	83	O(33)	4757(9)	3085(7)	-3434(10)	82
P(1)A	8332(3)	7119(2)	2876(4)	64	O(34)	5444(10)	3875(7)	-4396(10)	92
P(2)A	10726(3)	6276(2)	2398(3)	51	O(41)	11324(15)	3704(11)	2183(15)	153
P(1)B	3369(2)	6888(2)	-767(2)	31	O(42)	10661(20)	2732(15)	2506(22)	233
P(2)B	5208(2)	7325(2)	-2146(2)	29	O(43)	9765(15)	3521(11)	1308(16)	165
P(1)C	1014(3)	10285(2)	2965(3)	48	O(44)	11073(20)	2800(14)	881(71)	220
P(2)C	3405(3)	9154(2)	3713(3)	47	O(51)	6544(14)	9864(10)	2312(15)	142
N(1)A	9200(10)	6564(7)	5243(10)	64	O(52)	6933(14)	9378(10)	748(15)	151
N(2)A	11314(8)	5854(6)	4768(9)	49	O(53)	6316(16)	10614(12)	791(17)	174
N(1)B	3616(7)	5388(5)	-1802(7)	30	O(54)	7740(21)	10305(15)	1792(23)	241
N(2)B	5298(7)	5786(5)	-3053(7)	33					
N(1)C	1728(10)	10764(7)	1034(10)	68					
N(2)C	3954(10)	9673(7)	1685(10)	64					
C(1)A	7678(14)	7404(10)	4169(10)	82					
C(2)A	8352(17)	7931(12)	2063(18)	105					
C(3)A	7430(12)	6596(8)	1941(12)	59					
C(4)A	12076(18)	5876(13)	3155(19)	111					
C(5)A	10277(14)	5633(10)	1303(15)	78					
C(6)A	10965(15)	7105(11)	1683(16)	87					
C(7)A	8022(17)	6845(12)	4937(18)	103					
C(8)A	12046(15)	5490(11)	4114(16)	90					
C(1)B	2835(10)	6079(7)	-360(10)	43					
C(2)B	4031(11)	7303(8)	521(12)	54					
C(3)B	2217(11)	7617(8)	-1286(12)	56					
C(4)B	5898(10)	7008(7)	-3248(10)	42					
C(5)B	4418(11)	8227(8)	-2623(11)	51					
C(6)B	6186(11)	7597(8)	-1002(11)	53					
C(7)B	2632(9)	5573(7)	-1385(10)	38					
C(8)B	6240(10)	6135(7)	-3105(10)	41					
C(1)C	165(16)	10929(12)	1815(17)	96					
C(2)C	231(12)	9557(9)	3124(13)	65					
C(3)C	1043(19)	10829(14)	4249(20)	117					
C(4)C	4727(14)	8967(10)	3421(15)	80					
C(5)C	3621(14)	9537(10)	5129(14)	77					
C(6)C	2993(12)	8234(9)	3802(13)	61					
C(7)C	655(15)	10952(11)	928(15)	83					
C(8)C	4613(14)	8935(10)	2207(15)	83					
O(31)	3899(8)	4289(6)	-3804(8)	67					
O(32)	5457(8)	4084(6)	-2527(8)	63					

a) This parameter was used to define the origin of the unit cell along z and is listed without e.s.d.

trans-[RhBr₂(dmpe)₂]CF₃SO₃. This complex was prepared from trans-[RhCl₂(dmpe)₂]CF₃SO₃ and KBr by the same method as that described for *trans*(Br,Br),*cis*(P,P)-[RhBr₂(edmp)₂]⁺, and isolated as the trifluoromethanesulfonate. Yield: 39%. Found: C, 21.91; H, 4.58%. Calcd for [RhBr₂(dmpe)₂]CF₃SO₃=C₁₃H₃₂Br₂F₃O₃SP₄Rh: C, 21.93; H, 4.53%.

Crystal Structure Determination. Experimental conditions and refinement informations are listed in Table 1. For *trans*(Cl,Cl),*cis*(P,P)-[RhCl₂(edmp)₂]⁺, structure analysis of the PF₆ salt (**2a**) was also performed, because the structure of the ClO₄ salt (**2b**) could not be determined accurately ($P\bar{1}$, $Z=6$, $R=0.070$). Intensities were measured to $2\theta=55^\circ$ using graphite monochromatized Mo $K\alpha$ radiation ($\lambda=0.71073$ Å) on a Rigaku four-circle diffractometer AFC-5. The θ - 2θ scan technique was employed at a scan rate of 6°min^{-1} in θ . Lattice constants were determined from 14–36 2θ values ($20 < 2\theta < 30$). Absorption corrections were made by the numerical Gauss-integration method⁶ for polyhedral crystals and by utilizing the correction factors⁷ for a spherical sample. Systematic absences of

I indicate that the space group is *Pna*2₁ (No. 33) or *Pnam* [*a*cb setting of *Pnma* (No. 62)]. Since $Z=4$ and the complex cation is chiral, the space group was determined to be *Pna*2₁. The structure was difficult to solve because Rh and all Br atoms nearly lie on the glide plane at $y=1/4$ or $y=3/4$ (see Fig. 3). Position of the Rh atom was obtained from E map, and coordinated P and N atoms were located in the weighted Fourier synthesis. The structure of **2a** was solved by the heavy atom method. C(7) atom in the edmp ligand is disordered (see Fig. 5). The population parameters of two possible positions A and B were estimated to be 0.5. All the non-hydrogen atoms were refined anisotropically. The 7 hydrogen atoms among 36 in **1** and 11 among 30 in **2a** were located by the difference synthesis and others were calculated. Before the structure determination of **2a** was carried out, the structure of **2b** had been determined. The positions of the three independent Rh atoms obtained from the E map were confirmed by Patterson function. The other non-hydrogen atoms were located by Fourier syntheses. In order to reduce the number of parameters, C, N, and O atoms were refined isotropically and H atoms were not

included in the refinement. The structure of **3** was solved by Patterson-Fourier method. There exists structural disorder in the dmpe chelate rings (see Fig. 8). The thermal ellipsoids of the carbon atoms in the P-C-C-P moieties were unusually elongated perpendicular to the chelate ring with B_{eq} values 12–22 Å², and the five-membered chelate rings were almost flat with unrealistic C-C bond length of 1.30(1) Å. The split atom model was not introduced for this complex, because several possible conformations could be assigned to the five-membered rings and appropriate positions of the methyl groups corresponding to each conformation should be taken into account. Such a procedure would lead to equivocal results. Fortunately, the positions of the P atoms do not seem to be affected severely by the disorder. Complex neutral-atom scattering factors were used.⁸⁾ The calculations were carried out on a FACOM M380R computer at Keio University with the computation program system UNICS-III.⁹⁾ The function, $\sum w||F_o| - |F_c||^2$ was minimized by block-diagonal least squares. The final atomic parameters are listed in Table 2 and the bond lengths and bond angles within the complex cations in Table 3.¹⁰⁾

Table 3. Bond Lengths (l/Å)
and Bond Angles (φ/°)

1			
Rh-P(1)	2.288(3)	P(2)-C(7)	1.797(13)
Rh-P(2)	2.279(3)	P(3)-C(9)	1.790(15)
Rh-P(3)	2.282(4)	P(3)-C(10)	1.816(16)
Rh-N(1)	2.193(11)	P(3)-C(11)	1.825(14)
Rh-N(2)	2.155(12)	N(1)-C(4)	1.468(18)
Rh-N(3)	2.166(11)	N(2)-C(8)	1.539(18)
P(1)-C(1)	1.794(17)	N(3)-C(12)	1.477(18)
P(1)-C(2)	1.814(14)	C(3)-C(4)	1.500(21)
P(1)-C(3)	1.826(14)	C(7)-C(8)	1.531(21)
P(2)-C(5)	1.801(15)	C(11)-C(12)	1.540(21)
P(2)-C(6)	1.798(16)		
P(1)-Rh-P(2)	94.9(1)	Rh-P(2)-C(5)	121.2(5)
P(1)-Rh-P(3)	96.7(1)	Rh-P(2)-C(6)	119.3(5)
P(1)-Rh-N(1)	82.6(3)	Rh-P(2)-C(7)	102.5(4)
P(1)-Rh-N(2)	94.1(3)	C(5)-P(2)-C(6)	102.0(7)
P(1)-Rh-N(3)	168.9(3)	C(5)-P(2)-C(7)	102.7(6)
P(2)-Rh-P(3)	94.6(1)	C(6)-P(2)-C(7)	107.3(7)
P(2)-Rh-N(1)	168.4(3)	Rh-P(3)-C(9)	116.2(5)
P(2)-Rh-N(2)	84.2(3)	Rh-P(3)-C(10)	121.9(5)
P(2)-Rh-N(3)	96.1(3)	Rh-P(3)-C(11)	102.5(4)
P(3)-Rh-N(1)	96.9(3)	C(9)-P(3)-C(10)	105.5(7)
P(3)-Rh-N(2)	169.2(3)	C(9)-P(3)-C(11)	104.4(6)
P(3)-Rh-N(3)	83.0(3)	C(10)-P(3)-C(11)	104.4(7)
N(1)-Rh-N(2)	84.8(4)	Rh-N(1)-C(4)	111.8(8)
N(1)-Rh-N(3)	86.5(4)	Rh-N(2)-C(8)	110.9(8)
N(2)-Rh-N(3)	86.5(4)	Rh-N(3)-C(12)	112.6(8)
Rh-P(1)-C(1)	121.3(5)	P(1)-C(3)-C(4)	109.5(10)
Rh-P(1)-C(2)	118.4(5)	N(1)-C(4)-C(3)	109.4(12)
Rh-P(1)-C(3)	102.2(5)	P(2)-C(7)-C(8)	109.6(9)
C(1)-P(1)-C(2)	103.7(7)	N(2)-C(8)-C(7)	108.0(11)
C(1)-P(1)-C(3)	104.6(7)	P(3)-C(11)-C(12)	105.5(10)
C(2)-P(1)-C(3)	104.5(6)	N(3)-C(12)-C(11)	109.3(11)
2a			
Rh-Cl(1)	2.3323(13)	N(1)-C(7)A	1.532(9)
Rh-Cl(2)	2.3484(14)	N(2)-C(8)	1.487(7)
Rh-P(1)	2.2547(10)	P-F(1)	1.586(4)
Rh-P(2)	2.2494(17)	P-F(2)	1.554(4)
Rh-N(1)	2.162(4)	P-F(3)	1.578(4)

Rh-N(2)	2.168(3)	P-F(4)	1.517(5)
P(1)-C(1)	1.821(6)	P-F(5)	1.585(3)
P(1)-C(2)	1.793(5)	P-F(6)	1.568(4)
P(1)-C(3)	1.800(6)	C(1)-C(7)A	1.445(10)
P(2)-C(4)	1.829(5)	C(4)-C(8)	1.500(6)
P(2)-C(5)	1.814(6)	N(1)-C(7)B	1.456(11)
P(2)-C(6)	1.805(5)	C(1)-C(7)B	1.480(11)
Cl(1)-Rh-Cl(2)	173.33(5)	C(5)-P(2)-C(6)	103.6(2)
Cl(1)-Rh-P(1)	91.37(4)	Rh-N(1)-C(7)A	111.2(3)
Cl(1)-Rh-P(2)	90.20(5)	Rh-N(2)-C(8)	112.9(3)
Cl(1)-Rh-N(1)	87.50(10)	F(1)-P-F(2)	88.8(2)
Cl(1)-Rh-N(2)	88.37(8)	F(1)-P-F(3)	90.1(2)
Cl(2)-Rh-P(1)	92.23(4)	F(1)-P-F(4)	176.6(2)
Cl(2)-Rh-P(2)	94.77(5)	F(1)-P-F(5)	87.4(2)
Cl(2)-Rh-N(1)	87.29(10)	F(1)-P-F(6)	88.1(2)
Cl(2)-Rh-N(2)	87.76(8)	F(2)-P-F(3)	93.5(2)
P(1)-Rh-P(2)	98.91(5)	F(2)-P-F(4)	93.8(2)
P(1)-Rh-N(1)	84.16(10)	F(2)-P-F(5)	89.6(2)
P(1)-Rh-N(2)	177.20(8)	F(2)-P-F(6)	176.9(2)
P(2)-Rh-N(1)	176.22(11)	F(3)-P-F(4)	91.8(2)
P(2)-Rh-N(2)	83.88(9)	F(3)-P-F(5)	175.9(2)
N(1)-Rh-N(2)	93.04(12)	F(3)-P-F(6)	86.9(2)
Rh-P(1)-C(1)	102.4(2)	F(4)-P-F(5)	90.5(2)
Rh-P(1)-C(2)	118.6(2)	F(4)-P-F(6)	89.2(2)
Rh-P(1)-C(3)	117.8(2)	F(5)-P-F(6)	89.8(2)
C(1)-P(1)-C(2)	104.3(2)	P(1)-C(1)-C(7)A	112.0(5)
C(1)-P(1)-C(3)	107.5(2)	P(2)-C(4)-C(8)	107.9(3)
C(2)-P(1)-C(3)	105.0(2)	N(1)-C(7)A-C(1)	111.0(6)
Rh-P(2)-C(4)	100.8(2)	N(2)-C(8)-C(4)	108.5(4)
Rh-P(2)-C(5)	118.1(2)	Rh-N(1)-C(7)B	113.7(5)
Rh-P(2)-C(6)	120.2(2)	P(1)-C(1)-C(7)B	112.6(5)
C(4)-P(2)-C(5)	107.6(2)	N(1)-C(7)B-C(1)	113.3(7)
C(4)-P(2)-C(6)	105.3(2)		
3			
Rh-Cl(1)	2.359(2)	P(2)-C(8)	1.765(8)
Rh-Cl(2)	2.357(2)	P(2)-C(9)	1.785(10)
Rh-P(1)	2.335(1)	P(3)-C(4)	1.755(15)
Rh-P(2)	2.341(2)	P(3)-C(10)	1.781(12)
Rh-P(3)	2.335(1)	P(3)-C(11)	1.794(10)
Rh-P(4)	2.337(2)	P(4)-C(5)	1.790(9)
P(1)-C(2)	1.782(11)	P(4)-C(12)	1.797(8)
P(1)-C(6)	1.786(8)	P(4)-C(13)	1.787(11)
P(1)-C(7)	1.805(10)	C(2)-C(3)	1.300(13) ^{a)}
P(2)-C(3)	1.813(9)	C(4)-C(5)	1.292(16) ^{a)}
Cl(1)-Rh-Cl(2)	179.8(1)	C(6)-P(1)-C(7)	101.5(4)
Cl(1)-Rh-P(1)	89.9(1)	Rh-P(2)-C(3)	107.5(3)
Cl(1)-Rh-P(2)	90.3(1)	Rh-P(2)-C(8)	119.4(3)
Cl(1)-Rh-P(3)	90.9(1)	Rh-P(2)-C(9)	119.2(3)
Cl(1)-Rh-P(4)	90.3(1)	C(3)-P(2)-C(8)	102.2(4)
Cl(2)-Rh-P(1)	90.2(1)	C(3)-P(2)-C(9)	103.5(4)
Cl(2)-Rh-P(2)	89.6(1)	C(8)-P(2)-C(9)	102.7(4)
Cl(2)-Rh-P(3)	89.0(1)	Rh-P(3)-C(4)	104.8(5)
Cl(2)-Rh-P(4)	89.8(1)	Rh-P(3)-C(10)	120.2(4)
P(1)-Rh-P(2)	84.0(1)	Rh-P(3)-C(11)	117.4(3)
P(1)-Rh-P(3)	179.2(1)	C(4)-P(3)-C(10)	107.7(6)
P(1)-Rh-P(4)	95.4(1)	C(4)-P(3)-C(11)	108.0(6)
P(2)-Rh-P(3)	96.2(1)	C(10)-P(3)-C(11)	99.1(5)
P(2)-Rh-P(4)	179.1(1)	Rh-P(4)-C(5)	107.6(3)
P(3)-Rh-P(4)	84.4(1)	Rh-P(4)-C(12)	118.8(3)
Rh-P(1)-C(2)	106.7(3)	Rh-P(4)-C(13)	117.9(4)
Rh-P(1)-C(6)	117.8(3)	C(5)-P(4)-C(12)	103.5(4)
Rh-P(1)-C(7)	119.1(3)	C(5)-P(4)-C(13)	103.4(5)
C(2)-P(1)-C(6)	105.6(4)	C(12)-P(4)-C(13)	103.7(4)
C(2)-P(1)-C(7)	104.7(5)		

a) These short distances are unrealistic (see text).

Results and Discussion

***fac*-[Rh(edmp)₃]³⁺.** The addition of an excess of edmp to rhodium(III) chloride in ethanol yielded [Rh(edmp)₃]Cl₃. The complex was also obtained as a

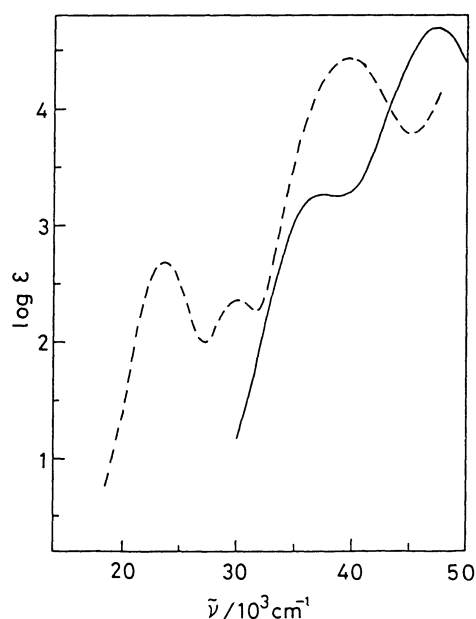


Fig. 1. Absorption spectra of *fac*-[Rh(edmp)₃]Cl₃·4H₂O in water (—) and *fac*-[Co(edmp)₃]Br₃·3H₂O in water (----).

by-product in the preparation of [RhCl₂(edmp)₂]⁺ from *mer*-[RhCl₃{P(*n*-Bu)₃}]₃ and edmp in benzene. The geometrical configuration of [Rh(edmp)₃]³⁺ is assigned on the basis of the ¹³C NMR spectrum. The complex in D₂O shows one, one, and two kinds of resonances for the NCH₂, PCH₂, and CH₃ groups, respectively. Thus the complex can be assigned to the *fac*(C₃) configuration, and the assignment was confirmed by the X-ray structure determination (vide infra). Figure 1 compares the absorption spectrum of *fac*-[Rh(edmp)₃]³⁺ with that of *fac*-[Co(edmp)₃]³⁺ 2) and the data are given in Table 4. The lowest-energy absorption band at 37300 cm⁻¹ of the rhodium(III) complex can be assigned to the first d-d absorption band, ¹A_{1g}→¹T_{1g}(O_h). The band is at higher energy by 13600 cm⁻¹ than the corresponding band of the cobalt(III) complex. The ratio of positions ($\tilde{\nu}_{\text{Rh}}/\tilde{\nu}_{\text{Co}}$) of the first absorption band for the complexes is 1.57. It should be noted that the value is very close to the spectrochemical parameter for rhodium(III), 1.56 given by Shimura (the parameter for cobalt(III) is 1.00).¹¹⁾ The second d-d absorption band, ¹A_{1g}→¹T_{2g}(O_h) of *fac*-[Rh(edmp)₃]³⁺ is hidden by the charge-transfer bands. The strong band at 47400 cm⁻¹ may be assigned to the Rh-P charge-transfer transition, since such a strong band is not observed for [Rh(en)₃]³⁺ 2) (en=ethylenediamine) in this region.

Figure 2 shows a perspective view of the [Rh(edmp)₃]³⁺ ion (1). The complex has approxi-

Table 4. Absorption Spectral Data^{a)}

Complex	$\tilde{\nu}/10^3 \text{ cm}^{-1} (\log \epsilon)$
<i>fac</i> -[Rh(edmp) ₃]Cl ₃ ·4H ₂ O	37.3(3.27) 47.4(4.69)
<i>trans</i> (Cl,Cl), <i>cis</i> (P,P)-[RhCl ₂ (edmp) ₂]PF ₆	25.5(2.34) 37.7(3.59) 47.0(4.72)
<i>trans</i> (Br,Br), <i>cis</i> (P,P)-[RhBr ₂ (edmp) ₂]PF ₆	21(1.4) ^{b)} 24.2(2.32) 33.0(3.36) 42.6(4.62)
<i>trans</i> (I,I), <i>cis</i> (P,P)-[RhI ₂ (edmp) ₂]PF ₆	19(1.7) ^{b)} 22.3(2.40) 28.1(3.92) 37.0(4.53) 41(3.9) ^{b)}
<i>trans</i> -[RhCl ₂ (dmpe) ₂]CF ₃ SO ₃	25.9(2.42) 32.6(3.78) 43.0(4.61) 46(4.4) ^{b)}
<i>trans</i> -[RhBr ₂ (dmpe) ₂]CF ₃ SO ₃	24.5(2.15) ^{b)} 29.8(3.40) 35(3.75) ^{b)} 42.1(4.58)

a) Solvent:CH₃OH except for *fac*-[Rh(edmp)₃]Cl₃·4H₂O (H₂O). b) Shoulder.

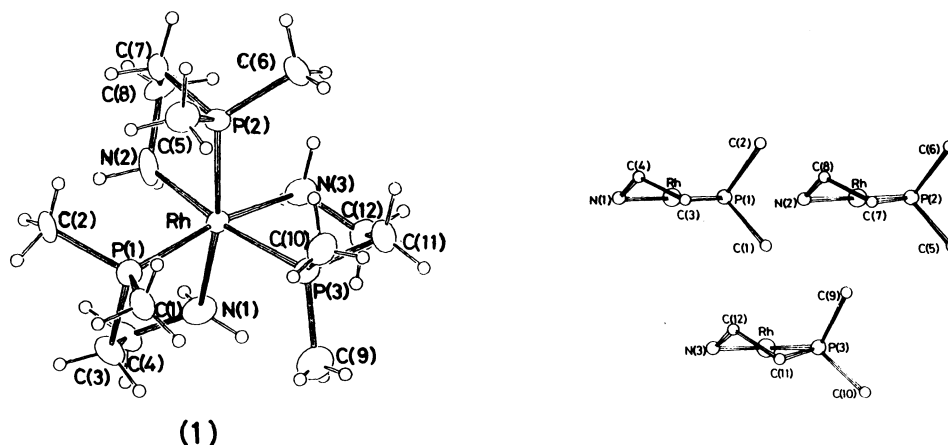
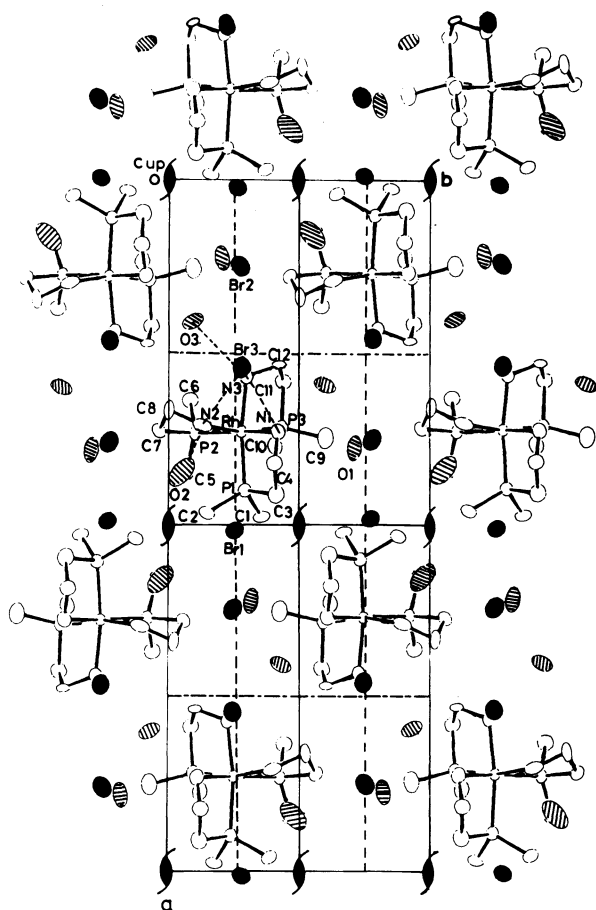


Fig. 2. A perspective view of *fac*-[Rh(edmp)₃]³⁺ (1) and edge-on views of the five-membered edmp chelate rings.

mate C_3 symmetry, and the P atoms are arranged in a facial manner as expected from the ^{13}C NMR spectrum. The C-C bonds in the chelate rings are nearly parallel to the pseudo- C_3 axis of the complex ion, and the complex can be designated as the lel_3 isomer. Three methyl groups C(1), C(5), and C(10) are disposed nearly parallel to the pseudo- C_3 axis. The short nonbonded C...C, C...H, and H...H distances among these methyl groups are 3.60(2)—3.70(2), 2.94(14)—3.03(14), and 2.33(17)—2.45(17) Å, respectively. The H...H repulsions are released by adjusting the mutual disposition of C-H bonds in the methyl groups. Such a crowded structure seems to be responsible for a distorted gauche conformation of the two edmp chelate rings (Fig. 2). In *fac-Δ*-[Co(edmp) $_3$] $^{3+}$, all three chelate rings take a pseudo (distorted) λ -gauche conformation.²⁾ The Rh-N distance averages 2.171(12) Å, which is significantly longer than that (2.062(7) Å) of [Rh(en) $_3$] $^{3+}$,¹³⁾ and that (2.076(4) Å) of *lel* $_3$ -[Rh(chxn) $_3$] $^{3+}$ ¹⁴⁾ (chxn=*trans*-1,2-cyclohexanediamine). The elongation of Rh-N distances can be attributed to the strong trans influence of the P donor atoms (*vide infra*). As seen from Fig. 3, the Br(3) atom lies approximately on the pseudo- C_3



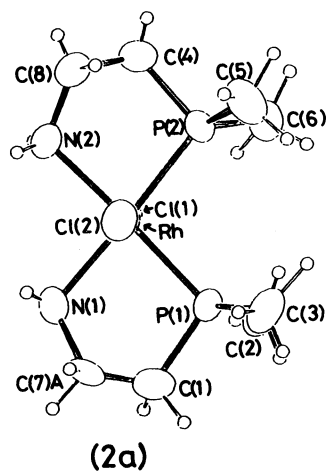


Fig. 5. A perspective view of $trans(Cl,Cl),cis(P,P)-[RhCl_2(edmp)_2]^+$ (**2a**) and edge-on views of the five-membered edmp chelate rings.

$[RhCl_2(edmp)_2]^+$ can be assigned to $trans(Cl,Cl),cis(P,P)$. The same structure was suggested by the absorption spectrum. Figure 4 compares the absorption spectrum of the complex with that of $trans(Cl,Cl),cis(P,P)-[CoCl_2(edmp)_2]^+$.¹⁷⁾ Both spectra are quite similar in pattern, although all of the bands of the rhodium(III) complex are shifted by 7500–9500 cm^{-1} toward higher energy compared to the corresponding bands of the cobalt(III) complex. Thus the rhodium(III) complex is suggested to have the $trans(Cl,Cl),cis(P,P)$ configuration. This assignment was confirmed by the X-ray structure determination (vide infra). The low-energy absorption band at 25500 cm^{-1} of the rhodium(III) complex can be assigned to the split component (I_a) of the first absorption band, $^1A_{1g} \rightarrow ^1T_{1g} (Oh)$. The I_a component is shifted toward higher energy by a factor of 1.5 on going from the cobalt(III) complex (16600 cm^{-1}) to the rhodium(III) complex (25500 cm^{-1}). The I_b and second absorption bands of the rhodium(III) complex are hidden by the strong charge-transfer bands.

Figure 5 shows a perspective drawing of the complex cation **2a**. **2a** is the $trans(Cl,Cl),cis(P,P)$ isomer, and the structure agrees with the assignment based on the ^{13}C NMR and absorption spectra. As illustrated in Fig. 5, one of the edmp chelate rings of **2a** is disordered. In **2b**, three independent complex ions take different conformations, $\delta\delta(\lambda\lambda)$, $\delta\lambda$, or $\delta(\lambda)$ envelope, suggesting flexibility of the edmp chelate rings (Fig. 6). The P(1)–Rh–P(2) angle of 98.91(5)° in **2a** is smaller than 105.4(1)° in $trans(Cl,Cl),cis(P,P)-[RhCl_2(edpp)_2]^+$,¹⁾ on account of less bulky substituents on phosphorus atoms. The mean Rh–N bond length in **2a**, 2.165(4) Å is longer than that in $trans-[RhCl_2(en)_2]NO_3$ (2.063(2) Å)¹⁸⁾ due to trans influence of the coordinated P atom. In Fig. 7, the M–N bond distance (M=Co or Rh) affected by the trans influence is plotted against the M–P bond distance. The elongation is smaller in the $trans(Cl,Cl),cis(P,P)-$

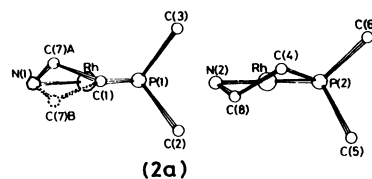


Fig. 6. Edge-on views of the five-membered edmp chelate rings in $trans(Cl,Cl),cis(P,P)-[RhCl_2(edmp)_2]-ClO_4$ (**2b**).

$[MCl_2(edpp)_2]^+$ complexes (circular symbols) than those in the others. This trend seems to be due to the longer M–P bond length in the edpp complexes. In general, the shorter the M–P bond length, the larger the M–N bond elongation. The elongations of the Rh–N bond distances (0.07–0.11 Å) by the trans influence are larger than those (0.03–0.07 Å) of the Co–N bond distances. Figure 7 clearly shows that the difference (<0.05 Å) between Rh–P and Co–P bond lengths is much smaller than that (ca. 0.1 Å) between Rh–N and Co–N bond lengths. All these results suggest a stronger affinity of P for Rh^{3+} than for Co^{3+} . The trans influence of P on the Rh–P bond length, the lengthening of mutually trans Rh–P bonds, was observed in the $trans-[RhCl_2(dmpe)_2]^+$ complex (**3**). The mean Rh–P bond distance is 2.337(2) Å, which is longer than those in complexes **1** and **2a**, 2.283(4) Å

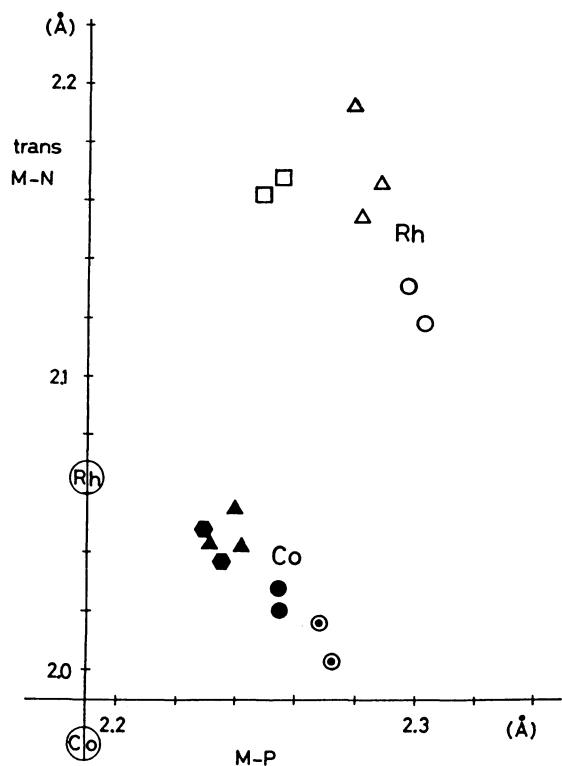


Fig. 7. Plot of the M-N distance (M=Co and Rh) against the trans M-P bond length in $\Delta=1$; $\square=2a$; $\circ=trans(Cl,Cl),cis(P,P)-[RhCl_2(edpp)_2]Cl \cdot 2C_2H_5OH$; $\blacktriangle=fac-[Co(edmp)_3]Br_3 \cdot 3H_2O$; $\bullet=trans(Cl,Cl),cis(P,P)-[CoCl_2(R-ebpp)_2]ClO_4$ ($R-ebpp=(R)-(2-aminoethyl)butylphenylphosphine$); $\bullet=trans(Cl,Cl),cis(P,P)-[CoCl_2(edpp)_2]1/2(CoCl_4)$; $\odot=trans(NCS,NCS),cis(P,P)-[Co(NCS)_2(edpp)_2]Br \cdot 3H_2O \cdot (CH_3)_2CO$.²⁵ The circles on the vertical axis indicate bond distances in the $[M(en)_3]^{3+}$ complexes (M=Co²⁶ and Rh¹³).

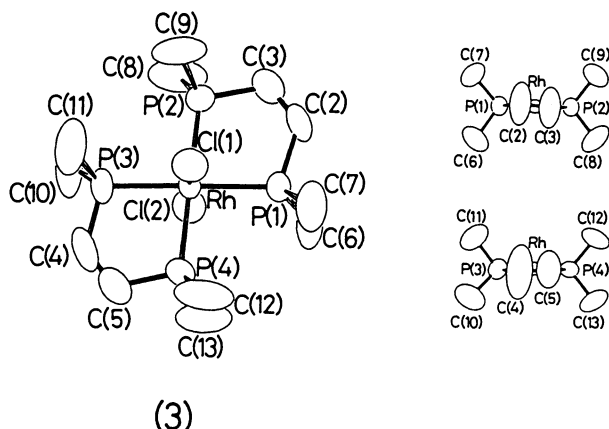


Fig. 8. A perspective view of $trans-[RhCl_2(dmpe)_2]^+$ (3) and edge-on views of the five-membered dmpe chelate rings.

and 2.252(2) Å, respectively.

$[RhCl_2(dmpe)_2]^+$ was prepared by refluxing an ethanol solution of $RhCl_3 \cdot 3H_2O$ and dmpe. Butter and Chatt reported that a mixture of the cis and trans

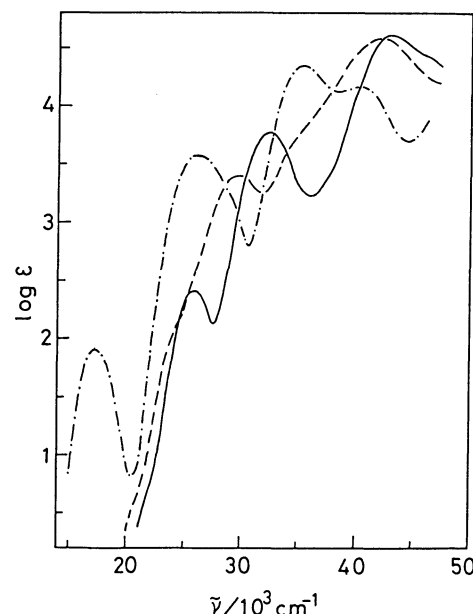


Fig. 9. Absorption spectra of $trans-[RhCl_2(dmpe)_2]-CF_3SO_3$ (—), $trans-[RhBr_2(dmpe)_2]CF_3SO_3$ (----), and $trans-[CoCl_2(dmpe)_2]ClO_4$ (-·-) in methanol.

isomers of this complex was yielded by a similar reaction.¹⁹ We obtained only one isomer, no fraction indicative of the other isomer being obtained in column chromatography. The structure was assigned to the trans isomer on the basis of the 1H NMR and absorption spectra, and the assignment was confirmed by X-ray analysis (Fig. 8). In the 1H NMR spectrum, the complex shows a similar spectral pattern to that of $trans-[CoCl_2(dmpe)_2]^+$.²⁰ The 1H NMR spectral pattern of $cis-[CoCl_2(dmpe)_2]^+$ is quite different from that of the trans isomer.²⁰ The absorption spectral pattern of $trans-[RhCl_2(dmpe)_2]^+$ is similar to that of the corresponding cobalt(III) complex; here also the ratio of positions ($\tilde{\nu}_{Rh}/\tilde{\nu}_{Co}$) of the I_a band for the rhodium(III) complex (25900 cm^{-1}) to that for the cobalt(III) complex (17300 cm^{-1})²⁰ is 1.5 (Fig. 9 and Table 4). The I_a band of $trans-[RhCl_2(dmpe)_2]^+$ is at higher energy (25900 cm^{-1}) than that of $trans(Cl,Cl),cis(P,P)-[RhCl_2(edmp)_2]^+$ (25500 cm^{-1}). The trans-dichloro rhodium(III) complexes of en, edpp, and Me_4-en ($=N,N,N',N'$ -tetramethylethylenediamine) show the I_a band at 24600,²¹ 24450,¹ and 22000 cm^{-1} ,²² respectively. Thus the spectrochemical series for the ligands can be determined as $dmpe > edmp > en \cong edpp > Me_4-en$. The same order has been reported for the trans-dichloro cobalt(III) complexes.^{17,20,23} $[RhX_2(edmp)_2]^+$ (X=Br, I) and $[RhBr_2(dmpe)_2]^+$ were prepared by substitution reactions from the trans-dichloro complexes and potassium bromide or sodium iodide. The configurations were retained in the reactions as indicated from the absorption spectra. The absorption spectra of $trans(X,X),cis(P,P)-[RhX_2(edmp)_2]^+$ (X=Cl, Br, I) are

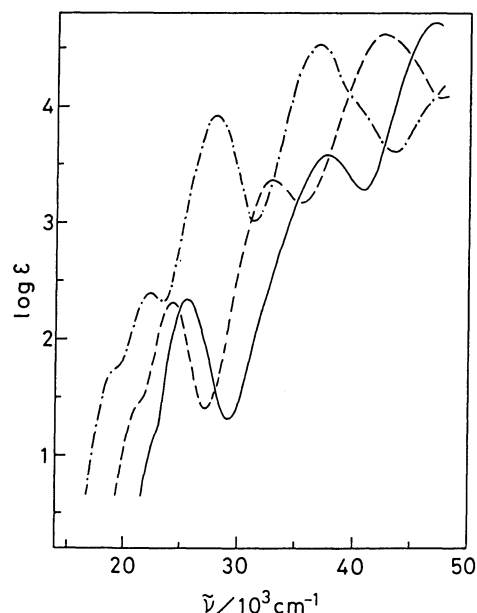


Fig. 10. Absorption spectra of *trans*(Cl,Cl),*cis*(P,P)-[RhCl₂(edmp)₂]PF₆ (—), *trans*(Br,Br),*cis*(P,P)-[RhBr₂(edmp)₂]PF₆ (---), and *trans*(I,I),*cis*(P,P)-[RhI₂(edmp)₂]PF₆ (— · —) in MeOH.

shown in Fig. 10. The spectral patterns of the complexes are similar to one another. In the series, the energy of the I_a component decreases in the order Cl > Br > I. The complexes show a shoulder at the low energy side of the I_a band and the absorption may be assigned to a spin-forbidden transition. The shoulder becomes more pronounced as X proceeds from Cl through Br to I. All of the complexes show two intense charge-transfer bands at energies higher than 28000 cm⁻¹. Both of the charge-transfer bands shift to lower energy in the order X = Cl > Br > I, suggesting that the bands are attributable mainly to the Rh-X charge-transfer transitions. In *trans*-[CoX₂(dmpe)₂]⁺ (X = Cl, Br, I), the positions of the Co-X charge-transfer transitions change in the same order²⁰ and in *trans*-[Co(H₂O)₂(dmpe)₂]⁺ they are missing.²⁴ Figure 9 shows the absorption spectra of *trans*-[RhX₂(dmpe)₂]⁺ (X = Cl, Br). The band at 32600 cm⁻¹ in the dichloro complex and the band at 29800 cm⁻¹ in the dibromo complex are assigned to the Rh-Cl and Rh-Br charge-transfer transitions, respectively. The bands are at lower energy than the corresponding bands in the edmp complexes, and the I_a component of *trans*-[RhBr₂(dmpe)₂]⁺ is observed as a shoulder by the overlap of the Rh-Br charge-transfer band. The intensity of this Rh-Br charge-transfer band (29800 cm⁻¹, log ε = 3.40) is remarkably smaller than that of the corresponding Rh-Cl charge-transfer band at 32600 cm⁻¹ (log ε = 3.78). The same trend is observed in many phosphine and arsine complexes of cobalt(III) and rhodium(III). The origin of the shoulder at ca. 35000 cm⁻¹ in the dibromo complex is unknown. The corresponding transition is not observed in the

dichloro complex, however, a similar transition is observed in *trans*-[CoBr₂(dmpe)₂]⁺.²⁰

Acknowledgement is made to Japanese Government (Monbusho) for providing generous fellowship support for K. P. S. to work as an exchange student at Nagoya University. We wish to thank Dr. Frode Galsbøl, University of Copenhagen, for helpful discussions and suggestions about our work. The present work was supported by a Grant-in-Aid for Scientific Research No. 61430013 from the Ministry of Education, Science and Culture.

References

- 1) F. Galsbøl, M. Kojima, T. Ishii, S. Ohba, Y. Saito, and J. Fujita, *Bull. Chem. Soc. Jpn.*, **59**, 1701 (1986).
- 2) I. Kinoshita, K. Kashiwabara, J. Fujita, K. Matsumoto, and S. Ooi, *Bull. Chem. Soc. Jpn.*, **54**, 2683 (1981).
- 3) S. A. Butter and J. Chatt, *Inorg. Synth.*, Vol. XIV, 185 (1974).
- 4) J. Chatt, N. P. Johnson, and B. L. Shaw, *J. Chem. Soc.*, **1964**, 2508.
- 5) G. M. Intille, *Inorg. Chem.*, **11**, 695 (1972).
- 6) W. R. Busing and H. A. Levy, *Acta Crystallogr.*, **10**, 180 (1957).
- 7) C. W. Jr. Dwiggin, *Acta Crystallogr., Sect. A*, **31**, 395 (1975).
- 8) "International Tables for X-ray Crystallography," Vol. IV, Kynoch Press, Birmingham (1974). (Present Distributor Kluwer Academic Publishers, Dordrecht.)
- 9) T. Sakurai and K. Kobayashi, *Rikagakukenkyusho Hokoku*, **55**, 69 (1979).
- 10) Tables of the coordinates of hydrogen atoms, the anisotropic thermal parameters of the non-hydrogen atoms, and observed and calculated structure factors are kept as Document No. 8901 at the Chemical Society of Japan.
- 11) Y. Shimura, *Bull. Chem. Soc. Jpn.*, **61**, 693 (1988).
- 12) F. Galsbøl, *Inorg. Synth.*, Vol. XII, 269 (1970).
- 13) A. Whuler, C. Brouty, P. Spinat, and P. Herpin, *Acta Crystallogr., Sect. B*, **32**, 2238 (1976).
- 14) H. Miyamae, S. Sato, and Y. Saito, *Acta Crystallogr., Sect. B*, **33**, 3391 (1977).
- 15) D. A. Redfield, L. W. Cary, and J. H. Nelson, *Inorg. Chem.*, **14**, 50 (1975).
- 16) P. S. Pregosin and R. W. Kunz, "³¹P and ¹³C NMR of Transition Metal Phosphine Complexes," Springer-Verlag, New York (1979), p. 65.
- 17) I. Kinoshita, Y. Yokota, K. Matsumoto, S. Ooi, K. Kashiwabara, and J. Fujita, *Bull. Chem. Soc. Jpn.*, **56**, 1067 (1983).
- 18) T. Lynde-Kernell and E. O. Schlemper, *Acta Crystallogr., Sect. C*, **44**, 31 (1988).
- 19) S. A. Butter and J. Chatt, *J. Chem. Soc. A*, **1970**, 1411.
- 20) T. Ohishi, K. Kashiwabara, and J. Fujita, *Bull. Chem. Soc. Jpn.*, **60**, 575 (1987).
- 21) H. Ogino and J. C. Bailar, Jr., *Inorg. Chem.*, **17**, 1118 (1978); S. A. Johnson and F. Basolo, *Inorg. Chem.*, **1**, 925 (1962).
- 22) G. W. Watt and P. W. Alexander, *J. Am. Chem. Soc.*, **89**, 1814 (1967).

23) M. Atoh, I. Kinoshita, K. Kashiwabara, and J. Fujita, *Bull. Chem. Soc. Jpn.*, **55**, 3179 (1982).

24) T. Ohishi, K. Kashiwabara, and J. Fujita, *Bull. Chem. Soc. Jpn.*, **60**, 583 (1987).

25) M. Atoh, K. Kashiwabara, H. Ito, T. Ito, and J. Fujita, *Bull. Chem. Soc. Jpn.*, **57**, 3139 (1984).

26) M. Iwata, K. Nakatsu, and Y. Saito, *Acta Crystallogr., Sect. B*, **25**, 2562 (1969).
